Optimizing Order to Minimize Low-Pass Filter Lag

Fredrik Dessen

Submitted: 2018-03-17 / Revised: 2018-06-05

Abstract This paper develops a tool kit for designing low-pass filters to exhibit the smallest possible phase drop. Based solely on the stopband requirements, it is thus possible to find the best order for a filter to be employed in a feedback loop. That is shown for two much-used filter families, Butterworth and Bessel, in cases where the filter is specified to have a minimum attenuation above a certain frequency. It is argued that the phase drop can be represented by an equivalent filter delay. Design tools are then developed, which do not depend on the precise dynamics of the application process. The tools comprise not only the means for determining the optimal filter order and bandwidth, but also formulae and tables useful for obtaining the resulting filter delay. A simple approximation is subsequently developed, which links the minimum obtainable delay directly to said requirements. The filter order needs not be known to apply this expression, and the filter family is represented in it by no more than a single constant. This rule of thumb is finally adapted to the area of anti-aliasing filters, and there briefly compared to approximative formulae found in existing literature.

Keywords Feedback systems · filter design · low-pass filters · minimum delay · optimal filter order · stopband attenuation

---

This work was supported in part by ENERSENSE, a strategic research program at NTNU.

F. Dessen
Norwegian University of Science and Technology (NTNU)
Division of Engineering Cybernetics
Tel.: +47-73412787
E-mail: fredrik.dessen@ntnu.no
ORCID: 0000-0002-6907-5057

1 Introduction

A low-pass filter has the distinct purpose of letting the low-frequency components of a signal pass undisturbed, while blocking high-frequency components. Indeed, texts on the subject, such as [1,3,5,8,10], often start by describing an ideal filter where signal components below a specified frequency are let through undisturbed, whereas those above this frequency are completely blocked. As a second, more realistic step, a model for the specification of an approximation is depicted. There, the filter attenuation in the stopband is constrained to be larger than some $D_s \gg 1$, and at the same time the attenuation in the passband to be smaller than some $D_d \gtrsim 1$. In this context, the stopband is defined as the set of frequencies above a specified value ω_s, and the passband as the set below some $\omega_d < \omega_s$. A comprehensive collection of design tools is available for solving this problem, aiming at a best-possible approximation of the ideal amplitude characteristics. These tools do not consider the phase shift of the filter, however.

In a feedback loop, the preservation of the gain in the passband is of secondary importance. Taking classical control theory as an example, serial compensation is applied in order to maximize the loop gain in the effective frequency range—not to keep it constant. At the same time, the stability of the closed-loop system is secured by manipulating the open-loop transfer function in the crossover region. This is the region encompassing the *phase crossover frequency* ω_{180}, where the phase drops below $-180°$, as well as the *gain crossover frequency* ω_c, where the gain passes 0 dB. The latter also defines the bandwidth of the loop. The insertion of a low-pass filter will reduce ω_{180}, and in turn prompt a reduction in ω_c in order to uphold the stability margin. The significance of phase in the design of low-pass filters for feedback loops is acknowledged and treated e.g. in [2,4,11]. They do not provide clear recommendations for what filter order to use in a specific situation, however. Design procedures with this feature seem hard to come by.

This paper develops and presents a set of design tools for filters in feedback loops. Sec. 2 builds the case by reviewing the established design process for the well-known and conceptually simple Butterworth low-pass filter, and points out how this approach influences the phase. This hopefully clarifies requirements, and supports the idea that, in the given context, the best filter order can be found from nothing more than the specified stopband attenuation. Sec. 3 puts forward that, in many cases, it can be sufficient to define optimality in terms of an equivalent delay rather than a more general functional. Based on this, tables of concrete and immediately usable optimal solutions for the Butterworth filter are developed. The extension to a second filter family is covered in Sec. 4. As is shown there, similar results are obtained for the Bessel filter. The above suggestions and findings are discussed in Sec. 5. In the same place, two approximative formulae for the preliminary assessment of filter performance are presented—as well as a complete filter design procedure. Sec. 6 concludes the paper by formulating rules of thumb specifically for anti-aliasing filters, and comparing them to the existing literature.

For a specific frequency ω_s,
  For each attenuation $D_s = 10$ dB through 90 dB,
    Start a separate diagram.
    For filter orders $n = 1$ through 10,
      Compute bandwidth ω_0.
      Add Bode plot of corresponding filter.

Fig. 1 Procedure used to generate Bode plots of low-pass filters

2 Butterworth Filters

The Butterworth filter is often defined by its attenuation as a function of frequency ω:

$$U_n(\omega) = \sqrt{1 + \left(\frac{\omega}{\omega_0}\right)^{2n}} \ . \tag{1}$$

Here, natural number n denotes the filter order, and ω_0 what is often called the bandwidth—or the cut-off or corner frequency. It is easily seen that $U_n(\omega_0) = \sqrt{2}$, approximately 3 dB, for any filter order n. The Butterworth filter is popular because of its maximally flat amplitude characteristics in the passband, as well as its conceptual simplicity. Both features serve well in this introductory example.

Traditionally [1, 7, 10] the filter order and bandwidth are found by first specifying a stopband in terms of the minimum attenuation D_s for frequencies above ω_s, and condensing this into requirement

$$U_n(\omega_s) = D_s \ . \tag{2}$$

The bandwidth is now found from (1) and (2) to be

$$\omega_0 = \omega_s \sqrt[-2n]{D_s^2 - 1} \ . \tag{3}$$

Subsequently, n can be negotiated so that ω_0 is arbitrarily close to ω_s. A closed-form expression for n is also available [7, 8, 10]:

$$n \geq \frac{\log \frac{D_s^2 - 1}{D_d^2 - 1}}{2 \log \frac{\omega_s}{\omega_d}} \ . \tag{4}$$

Here, the passband specification outlined in the introduction is used. Bandwidth ω_0 can still be found from (3).

A preliminary investigation for different stopband specifications, with ω_0 found from (3), can be carried out according to the procedure shown in Fig. 1. Amplitude and phase characteristics produced for a range of filter orders, all having the same specified attenuation at the same specified frequency, are shown in Fig. 2.

As can be seen from this representative sample, a specific order (in this case $n = 5$) appears to cause the smallest phase drop in most of the passband. Diagrams for the remaining values of D_s are shown in Online Resource 1. These

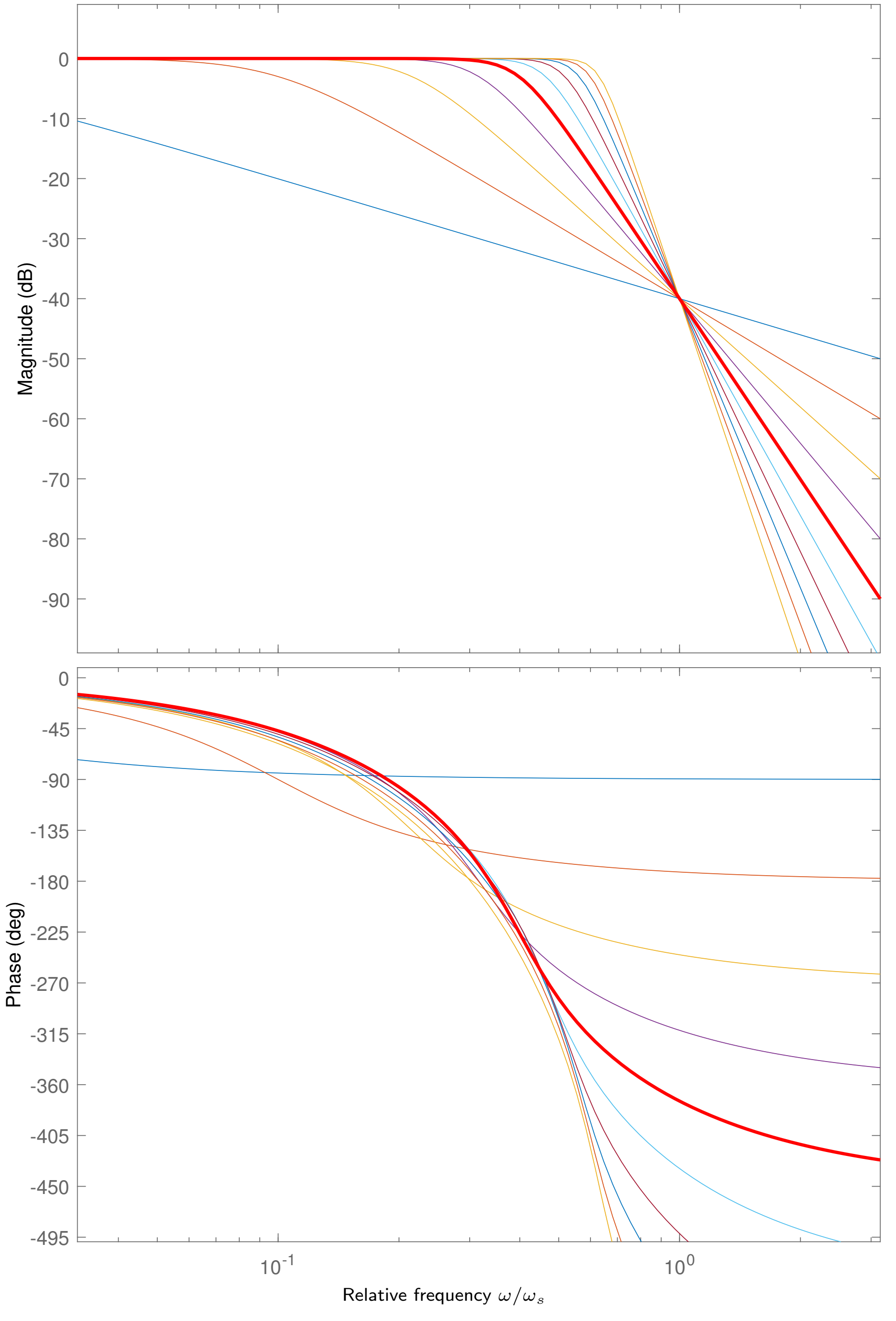

Fig. 2 Bode plots of Butterworth filters of orders 1 through 10. Order 5 is highlighted, since it features the smallest phase drop. All filters have the same attenuation of 40 dB at $\omega = \omega_s$

Table 1 Optimal filter order

D_s[dB]	10	20	30	40	50	60	70	80	90
n	2	3	4	5	6	7	8	9	10

Best order n of Butterworth or Bessel filters for different stop band attenuations D_s, as determined by visual inspection.

follow the same pattern, and the full range of plots reveals the remarkably clear correspondence summarized in Table 1.

This first takeaway suggests that, if a Butterworth low-pass filter is specified to have a certain minimum attenuation D_s in the stopband, a specific filter order n can be identified, which causes the smallest phase drop.

3 Filter Delay

The results in Table 1 rely on visual judgement. A properly posed minimization problem, however, is specified in terms of a single functional.

In a well-designed control system, the phase lag at gain crossover should be dominated by the process and the controller rather than the filter. According to [11], a phase drop of 5° to 15° due to the filter can be acceptable. Thus, when comparing phase lags caused by the filters themselves, it is probably not necessary to consider much greater values. Since small lags in this context imply low frequencies, it may be convenient to compare filters in terms of a single scalar describing phase in that end of the spectrum.

The signal-processing community are comfortable with the terms *group delay* and *phase delay*. Indeed, [4] for instance, in a section called *Filter delay*, uses the *low-frequency group delay* to compare the phase contribution of several filter types. In the same way; restricted to Bessel filters, however, [2] uses the term *approximate time delay* synonymously with the *zero-frequency delay* coined by Thomson in his paper [9]. The latter is adopted hereinafter, since, at sufficiently low frequencies, the group delay and phase delay values for the filters of interest turn out to be identical. The term will alternate with short hands *filter delay*, or simply *delay*.

Introducing s, the differential operator of the Laplace transform, the notion of a delay can be established by representing time shift $-\tau$ by transfer function

$$e^{-\tau s} = \frac{1}{1 + \tau s + \frac{1}{2}(\tau s)^2 + \cdots} \ . \tag{5}$$

Comparing this with the general, all-pole filter transfer function

$$H_n(s) = \frac{1}{A_n(s)} = \frac{1}{1 + a_{1,n}s + \cdots + a_{n,n}s^n} \ , \tag{6}$$

it is seen that, for sufficiently small values of s,

$$H_n(s) \approx e^{-a_{1,n}s} \ . \tag{7}$$

Alternatively, the zero-frequency delay can be depicted as the apparent steady state time shift in the ramp response of $H_n(s)$, which is readily obtained for instance by applying the final value theorem.

3.1 Zero-frequency delay of the Butterworth filter

Equation (1) also determines the transfer function of the filter,

$$H_n(s) = \frac{1}{B_n(\frac{s}{\omega_0})} \ . \tag{8}$$

Butterworth polynomials $B_n(x)$ are readily available in tables, such as in [3, 5, 10], usually in terms of constants $2\zeta_{k,n}$ of expression

$$B_n(x) = (1+x)(1+2\zeta_{1,n}x+x^2)\cdots(1+2\zeta_{m,n}x+x^2) \ . \tag{9}$$

Here, n is odd and $m \triangleq (n-1)/2$. If n is even,

$$B_n(x) = (1+2\zeta_{1,n}x+x^2)\cdots(1+2\zeta_{m,n}x+x^2) \ , \tag{10}$$

and $m \triangleq n/2$. The relative damping constants $\zeta_{k,n}$ are found [7, 10] from

$$\zeta_{k,n} = -\cos\frac{2k+n-1}{2n}\pi \quad \text{for all} \quad k \leq m \ . \tag{11}$$

The zero-frequency delay, by (7), is related to the first-degree coefficient of the expanded form

$$B_n(x) = 1 + b_{1,n}x + \cdots + b_{1,n}x^{n-1} + x^n \tag{12}$$

of (9) or (10). Inserting (11) into either, a compact, closed form for the first-degree coefficient is found as

$$b_{1,n} = -\sum_{k=1}^{n}\cos\frac{2k+n-1}{2n}\pi \ . \tag{13}$$

The zero-frequency delay is now found from (7). Expanding shorthand x into s/ω_0 in (12), and then inserting (3), completes the sequence

$$\tau_n = a_{1,n} = \frac{b_{1,n}}{\omega_0} = \frac{b_{1,n}\sqrt[2n]{D_s^2-1}}{\omega_s} \ . \tag{14}$$

Sample values of the relative delay

$$\omega_s\tau_n = b_{1,n}\sqrt[2n]{D_s^2-1} \ , \tag{15}$$

for different combinations of n and D_s, are shown in Table 2. As can be seen: for each attenuation value D_s, a filter order n can be found, which exhibits the smallest delay.

Table 2 Butterworth filter delays

D_s	$n=2$	3	4	5	6	7	8	9	10	11
20 dB	4.4609	4.3017	4.6410	5.1237	5.6664	6.2399	6.8311	7.4336	8.0436	8.6589
30 dB	7.9507	6.3235	6.1959	6.4562	6.8702	7.3601	7.8929	8.4522	9.0291	9.6182
40 dB	14.1418	9.2830	8.2633	8.1286	8.3240	8.6764	9.1151	9.6062	10.1313	10.6799
50 dB	25.1486	13.6258	11.0194	10.2333	10.0849	10.2276	10.5260	10.9171	11.3676	11.8583
60 dB	44.7213	20.0000	14.6947	12.8830	12.2181	12.0559	12.1553	12.4069	12.7546	13.1667
70 dB	79.5271	29.3560	19.5957	16.2188	14.8026	14.2111	14.0367	14.1000	14.3109	14.6195
80 dB	141.421	43.0887	26.1313	20.4182	17.9337	16.7517	16.2093	16.0241	16.0571	16.2325
90 dB	251.487	63.2456	34.8466	25.7050	21.7272	19.7463	18.7182	18.2108	18.0164	18.0236

Relative delays $\omega_s \tau_n$ for filters of order $n = 2$ through 11 with $D_s = 20$ through 90 dB. The shortest delay for each specific attenuation is given a grey background. Multiple values are marked where they differ by less than 1%.

Table 3 Switching points for Butterworth filters

Order	1	2	3	4	5	6	7	8	9	10	11
Attenuation[a]		7.0	18.1	27.9	37.1	46.2	55.1	64.0	72.8	81.6	90.4

[a]) Values [dB] of attenuations $D_{s,n,n+1}$ separating optimal filter orders n and $n+1$.

3.2 Switching Points

Imagine that order n is optimal for some value of D_s. Thence, D_s is increased until a transition is made from order n being optimal to $n+1$ being optimal. At that point, both choices result in the same delay value,

$$\tau_n = \tau_{n+1} \ , \tag{16}$$

and (14) can be inserted twice into (16), which becomes

$$\frac{b_{1,n} \sqrt[2n]{D_s^2 - 1}}{\omega_s} = \frac{b_{1,n+1} \sqrt[2(n+1)]{D_s^2 - 1}}{\omega_s} \ . \tag{17}$$

This can be rearranged into

$$\frac{b_{1,n}}{b_{1,n+1}} = \frac{\sqrt[2(n+1)]{D^2{}_s - 1}}{\sqrt[2n]{D^2{}_s - 1}} = \sqrt[-2n(n+1)]{D^2{}_s - 1} \ , \tag{18}$$

and finally solved for D_s:

$$D_{s,n,n+1} = \sqrt{\left(\frac{b_{1,n}}{b_{1,n+1}}\right)^{-2n(n+1)} + 1} \ . \tag{19}$$

Here, the switching point is denoted by the more elaborate $D_{s,n,n+1}$ to emphasize that both n and $n+1$ are optimal. The expression depends on two b_1 values, both of which can be computed from (13). Table 3 shows the results obtained for a range of switching points, and is easily extended by continuing to apply (19) for as long as desired. The optimal filter order is thus easily found for any attenuation specified.

4 Bessel Filters

The Bessel filter is credited [2] with being the superior choice for anti-aliasing filters in high performance control systems, and is thus included herein. Its phase characteristics is designed to be as linear as possible for each filter order; consequently, the signal will pass with only a minimum of distortion. Step responses for instance, are shown in [6] to exhibit very little overshoot. Serving as a low-pass filter, however, its amplitude characteristics is rather poor. It was argued above that the latter is of reduced importance in the present context.

A Bessel filter of order n can be defined in terms of the all-pole transfer function

$$G_n(s) = \frac{1}{C_n(\tau s)} \ . \tag{20}$$

Starting with $c_{0,n} = c_{1,n} = 1$, the coefficients of polynomial C_n are found [7] from the recursion

$$c_{k+1,n} = \frac{2(n-k)}{(k+1)(2n-k)} c_{k,n} \ . \tag{21}$$

Expanding the denominator into

$$C_n(\tau s) = 1 + \tau s + c_{2,n}(\tau s)^2 + \cdots + c_{n,n}(\tau s)^n \ , \tag{22}$$

by (7), constant τ is immediately identified as the zero-frequency delay. However, finding the zero-frequency delay for a desired attenuation D_s at a specified frequency ω_s implies solving

$$D_s \ = |C_n(\tau s)| \tag{23}$$

for τ, with s set to $j\omega_s$. As is evident from Fig. 3, $|C_n(\cdot)|$ is monotonic. Thus, no complications should arise from solving (23), for instance by iteration.

The transfer function of the Bessel filter can be found using *Matlab Signal Processing Toolbox* function `besself`—or for instance, *Python* function `scipy.signal.bessel`. These take a different filter constant than τ, however: corner frequency ω_0, which marks the intersection of the low-frequency and high-frequency gain asymptotes. Thus, a conversion formula is needed. According to (22),

$$\lim_{\omega \to 0} |C_n(j\omega\tau)| = 1 \ , \tag{24}$$

whereas for high frequencies, (21) and (22) imply

$$\lim_{\omega \to \infty} |C_n(j\omega\tau)| = c_{n,n}(\omega\tau)^n = \frac{2^n n!}{(2n)!}(\omega\tau)^n \ . \tag{25}$$

Equating (24) and (25) and solving for ω yields corner frequency

$$\omega_0 = \frac{1}{\tau}\left(\frac{(2n)!}{2^n n!}\right)^{1/n} \ . \tag{26}$$

Table 4 Bessel filter delays

D_s	$n=2$	3	4	5	6	7	8	9	10	11
20 dB	5.3280	5.0771	5.3718	5.8301	6.3534	6.9039	7.4626	8.0183	8.5631	9.0915
30 dB	9.6609	7.6569	7.3901	7.5952	7.9897	8.4762	9.0123	9.5756	10.1532	10.7365
40 dB	17.2768	11.3556	9.9853	9.7059	9.8397	10.1704	10.6087	11.1110	11.6535	12.2216
50 dB	30.7763	16.7413	13.4007	12.3133	12.0242	12.1015	12.3749	12.7644	13.2277	13.7401
60 dB	54.7586	24.6212	17.9293	15.5683	14.6409	14.3444	14.3764	14.5997	14.9433	15.3670
70 dB	97.3927	36.1713	23.9517	19.6489	17.7928	16.9684	16.6658	16.6610	16.8407	17.1422
80 dB	173.201	53.1141	31.9714	24.7743	21.5992	20.0484	19.2957	18.9883	18.9528	19.0946
90 dB	308.005	77.9756	42.6577	31.2182	26.2018	23.6699	22.3228	21.6228	21.3115	21.2503

Relative delays $\omega_s \tau_n$ for filters of order $n = 2$ through 11 with $D_s = 20$ through 90 dB. The shortest delay for each specific attenuation is given a grey background. Multiple values are marked where they differ by less than 1%.

Table 5 Switching points for Bessel filters

Order	1	2	3	4	5	6	7	8	9	10	11
Attenuation[a]	8.5	17.4	26.2	34.9	43.7	52.4	61.1	69.8	78.5	87.2	

[a]) Values [dB] of attenuations $D_{s,n,n+1}$ separating optimal filter orders n and $n+1$.

A new investigation can now be carried out according to the procedure in Fig. 1: this time with ω_0 found by first solving (23) for τ and then applying (26). Fig. 3 shows Bode plots that are directly comparable to those in Fig. 2. A visual inspection of the phase plots indicates that, with D_s at 40 dB, the best phase is again found for $n = 5$. Diagrams for the remaining values of D_s are found in Online Resource 2. These follow the same pattern, and the full range of plots suggests that Table 1 is valid for Bessel as well as for Butterworth filters. The zero-frequency delays are found in the process, and the new set of relative delays are shown in Table 4.

Switching points are found using the same argumentation as with the Butterworth filter. Defining shorthand $x \triangleq \omega\tau$, (23) can be squared and written

$$D_s^2 = (1 - c_{2,n}x^2 + c_{4,n}x^4 - c_{6,n}x^6 + \cdots)^2 + (x - c_{3,n}x^3 + c_{5,n}x^5 - \cdots)^2 \ , \quad (27)$$

but also, for the next filter order,

$$D_s^2 = (1 - c_{2,n+1}x^2 + c_{4,n+1}x^4 - \cdots)^2 + (x - c_{3,n+1}x^3 + c_{5,n+1}x^5 - \cdots)^2 \ . \quad (28)$$

Following the reasoning leading to (16), for any natural number n, (27) and (28) can be combined and solved for x. The insertion of x back into either, produces Table 5, which settles the best order for a Bessel filter the same way as Table 3 does for a Butterworth filter.

5 Discussion

This paper describes principles for determining the filter constant and order of a low-pass filter, in situations where the minimum attenuation D_s above a certain frequency ω_s is specified. It argues that the traditional approach,

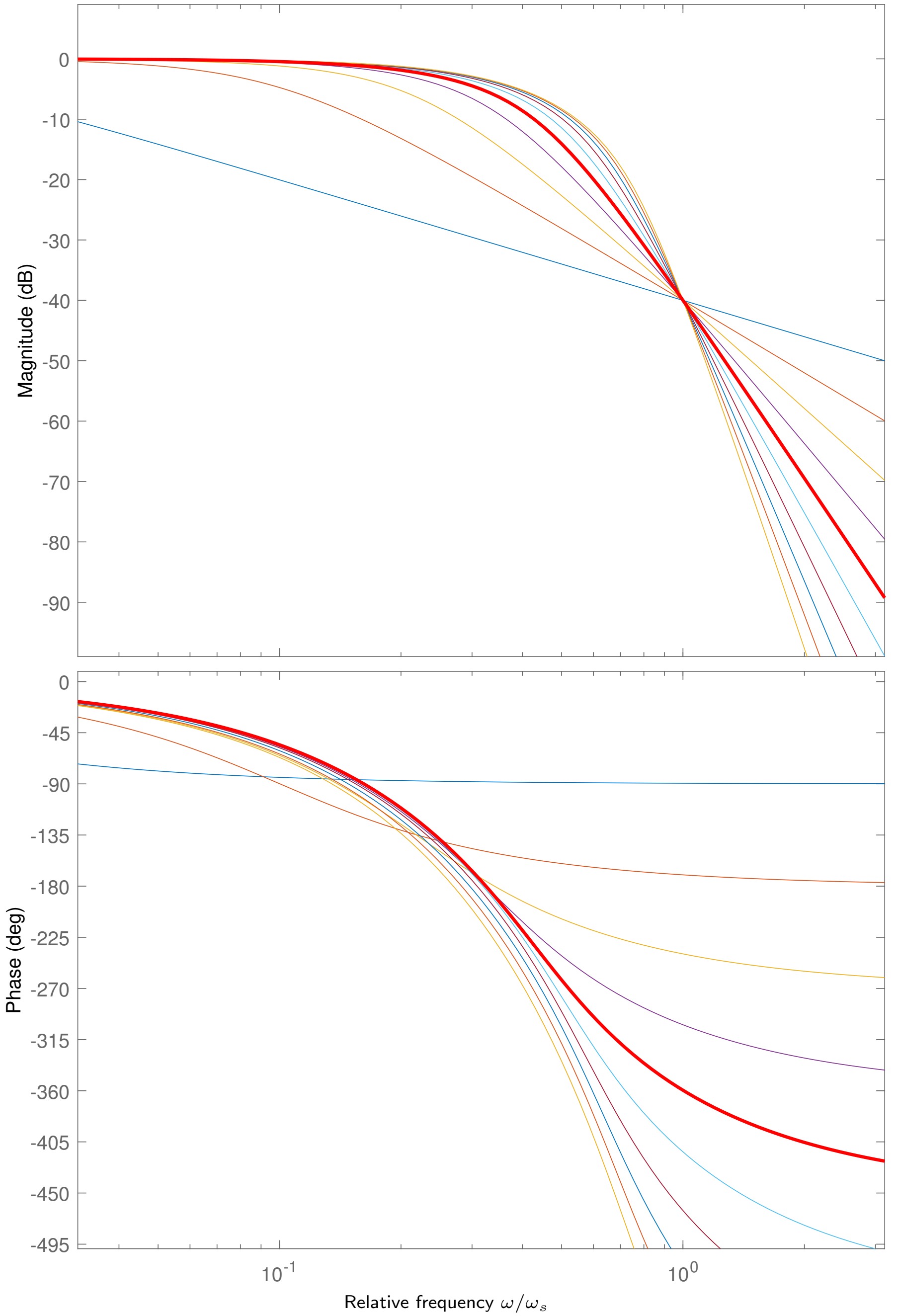

Fig. 3 Bode plots of Bessel filters of orders 1 through 10. Order 5 is highlighted, since it features the smallest phase drop. All filters have the same attenuation of 40 dB at $\omega = \omega_s$

represented by (4), for finding the best order of a low-pass filter is of limited value in cases where the filter lag needs to be minimized. It proceeds by developing better, still equally simple, rules for that scenario. Inspecting Bode plots of Butterworth and Bessel filters over a range of orders leads to the easily memorized Table 1.

5.1 Investigating the tables

The *zero-frequency delay* is proposed as a scalar measure for comparing filters, and is displayed in Table 2 for the Butterworth filter. The results are in full agreement with Table 1. Table 4 as well is in good agreement with Table 1, except that the best order is elevated by one for D_s values of 60 dB and above. However, a closer look shows that the delay values corresponding to the filter orders of Table 1 are no more than 0.3% larger than the minimum values. Understandably, this difference is difficult to resolve by eyesight.

Tables 2 and 4 can be compared directly. In each table row, the shortest delay has been highlighted together with any entry deviating by less than 1% from it. As can be seen, the lowest order in each group is the same for both families. Thus, the difference between the results obtained by visual inspection, and those obtained by minimizing the zero-frequency delay, can probably be explained by taking into account the author's understandable bias towards lower filter orders. It can be concluded that the zero-frequency delay can be used with both filter families, and yields approximately the same results as a visual inspection.

It was argued above, that the zero-frequency delay only needs to represent the filter accurately for lags smaller than 15°. Nevertheless, for either filter family, the inspection of the Bode plots indicate that the validity range can be extended to include lags approaching 90°. This further corroborates the use of the zero-frequency delay in the present context.

With this established, Tables 3 and 5 can be said to form reliable, precomputed maps indicating which filter order to recommend for each specific situation. As can be seen, the switching points differ between the Butterworth and Bessel filters, but by no more than 3.2 dB. This difference hardly matters in practice. Nevertheless, now that both tables exist, there is little reason not accept them as they are.

Interestingly, in addition to the almost linear correspondence between the optimal order n and the decibel value of D_s, Tables 2 and 4 also reveal a nearly linear relationship with the minimum delay, which can be expressed as

$$R \cdot \omega_s \tau_{min} \approx 20 \log D_s \ . \tag{29}$$

The tables indicate that constant R is approximately 5 for a Butterworth and 4 for a Bessel filter. This makes it easy, quite early in a design process—and without caring about the exact filter order—to provide a direct relationship between the stopband requirements and the shortest obtainable delay.

Start with a specification of the stopband in terms of ω_s and D_s, considering for instance (29) and (30). With a Butterworth filter, the remaining steps are:

1. Use Table 3 to find the optimal filter order n for the specified attenuation D_s.
2. Obtain filter parameter ω_0 from (3). Optionally, apply (13) and (14) to find the exact zero-frequency delay τ.

The order of a Bessel filter is equally easy to obtain. Finding the filter constant is slightly more laborious, however:

1. Use Table 5 to find the optimal filter order n for the specified attenuation D_s.
2. Solve (23) for the exact filter delay τ, and apply (26) to find ω_0 if desired.

One way to solve (23) is by interpolation in the relevant column of Table 4. On top of this, if needed, the result can be further improved by iteration.

Fig. 4 Design procedure for low-pass filter in feedback loop

Studying Tables 2 and 4, it is also noted that each column therein represents a tabulated version of the relationship between stopband attenuation D_s and relative delay $\omega_s \tau_n$ for a specific filter order and family. Hence, solving (23) for τ can be reduced to the interpolation of the corresponding column of Table 4. This option is incorporated in the final design procedure.

5.2 Matching the application

Up to this point, considerations have remained comfortably detached from the application process. In the introduction, and with classical control theory as the example, it was pointed out that stability is linked to the gain and phase characteristics in the crossover region. A simple link to the dynamics in this region can thus be made through the approximation

$$\phi_c \approx \tau_{min} \omega_c \ , \tag{30}$$

which simply expresses the phase drop ϕ_c corresponding to delay τ_{min} at frequency ω_c. In principle, the latter can represent any frequency deemed significant by the engineer, but notably the gain crossover frequency of the loop transfer function. That way, (30) can for instance be considered together with the recommendation implied in [11] that the phase drop due to the filter should not exceed 15° at gain crossover. This, together with (29), can be used to negotiate a stopband specification.

The tools developed in this paper are brought together to form the design procedure outlined in Fig. 4. As can be seen, both filter families are incorporated. The emphasis on delay mitigation, and the fact that the Butterworth filter offers a 20% shorter delay than the Bessel filter, brings the former forward as the primary choice. On the other hand, the Bessel filter offers the most well behaved step response of the two, and is thus favored in [2, 11].

Though no claims are made regarding how well the filters serve as delay approximations, it has been demonstrated that any transfer function with the structure shown in (6) can be said to approximate a delay to some extent. In a Bode plot, the two hallmarks of a delay are *unity gain* and *linear phase*, and each of the two filter families investigated excel in one of these areas: the

Butterworth filter in the first, and the Bessel filter in the second [1, 10]. In a specific situation, if it matters that the filter is an accurate approximation of a delay, the system designer will still have to determine whether a maximally flat gain or a linear phase best serves its purpose. In the introduction to this paper, it is argued that the gain in the passband is of secondary importance. It needs to be pointed out, however, that a maximally flat gain can still be of value in some situations. There is even a chance that the designer will have to revisit (4) while negotiating the best solution for the problem at hand.

6 Anti-aliasing filters

Reasons for employing low-pass filters vary. One specific usage, that fits well in the present context, is the *anti-aliasing filter*. Its purpose is to prevent frequency content near or above the Nyquist frequency from entering a downstream, discrete-time processing unit. These filters comprise analog electronic circuitry; hence, they are kept reasonably simple. Their design procedure can also be held simple, since the downstream system usually does not need to be considered in any detail. Their employment in digital feedback systems comes highly recommended in [2, 4, 11], and defines a context in which comparisons to some degree can be made.

Approximations of phase as a function of stopband requirements are briefly presented in [2, 11]. These are useful for estimating the impact of specific filter parameters on the phase. Notably, the expressions therein are developed for specific filter orders. In contrast, the combination of (29) and (30) herein produces the alternative approximation

$$\phi_c \approx \frac{20 \log D_s}{R} \cdot \frac{\omega_c}{\omega_s} \ , \tag{31}$$

which for instance can be used to estimate the phase contribution from the filter at an anticipated gain crossover frequency ω_c. A similar relationship is formed by

$$\phi_c \approx \frac{20 \log D_s}{RS} h\omega_c \ , \tag{32}$$

with constant $S \triangleq h\omega_s$ imposing an inversely proportional relationship between sample period h and stop band limit ω_s. In line with the sampling theorem, it is recommended that $S \lesssim \pi$. Clearly, neither (31) nor (32) depend on the filter order. Instead, both implicitly assume the best choice.

In [2, Table 7.3], delays for Bessel filters of order 4 and 6 are presented for different stopband attenuations. The columns therein tabulate values of τ_n/h, which can be compared to corresponding values of $\tau_n\omega_s$ in Table 4 herein, simply by dividing the latter by $S = \pi$. The tables match, albeit with reduced accuracy at high attenuation values, consistent with the fact that the entries in the reference are admittedly approximations. The switching point between $n = 4$ and 6 being the best choice, appears to lie somewhere between $D_s = 34$

dB and 40 dB. This in no way contradicts Tables 4 and 5 herein. Nevertheless, the notion of an optimal filter order seems to go unnoticed in [2].

It is straightforward to extend (29) to establish a proportional approximative relationship between the smallest obtainable delay τ_{min} and the sample interval h of the controller:

$$\tau_{min} \approx \frac{20 \log D_s}{RS} h \ . \tag{33}$$

This delay can be compared with, and of course added to, the average processing delay τ_{con} of a controller with a zero-order hold element on its output. The relationship usually presented in the literature is

$$\tau_{con} \approx Eh \ , \tag{34}$$

with E typically being assigned the value 0.5 as in [11], or 1.5 as in [4], depending on the assumptions made regarding the digital controller.

A rule of thumb for the two delays is presented in [4, Eq. 10.4.2]. In agreement with (33) and (34), both are proportional to the sampling period. Notably, the filter delay therein is a linear function of its order. Consequently, that expression cannot capture the major point made herein: that the smallest delay will be found at some optimal filter order n. This, on the other hand, is implicit in (33).

A similar expression, this time in terms of phase lag at the crossover frequency, appears in the deliberations leading to [11, Eq. 36]. As should be, the result depends on stopband requirements through D_s. On the other hand, again, the expression is developed for a specific filter order, and is thus of limited use. In the present context, a similar approximation of the total phase lag can be obtained as an extension of (32) involving (34):

$$\phi_{tot} \approx (\tau_{min} + \tau_{con})\omega_c \approx (E + \frac{20 \log D_s}{RS}) h\omega_c \ . \tag{35}$$

Focus remains on the basic requirement: the stopband specification. Since the optimal filter order too is a function of D_s, it does not appear in (35).

7 Conclusion

It is tempting to round off by citing Elliot, who dedicates [4] *to all those whose theories become glaringly obvious in retrospect*: I just might qualify.

Still, the procedure outlined in Sec. 5.2, and summarized in Fig. 4, represents a practical and simple approach to filter design. As a supplement, (31) through (35) can be useful in the preliminary assessment of anti-aliasing filters, as well as in negotiating the sampling rate, or the closed-loop bandwidth, of the system. These tools can be of use even before finding the optimal filter order.

A foundation for the above is that the phase lag can be represented adequately through the zero-frequency delay. The discussion in Sec. 5.1 indicates that this is a reasonably sound assumption. A second footing is the need for minimizing the delay, subject to the basic stopband requirements presented in the introduction. Of course, the validity of this premise needs to be considered in each individual case.

From my perspective, giving undergraduate courses in control and instrumentation, there is an additional boon. The above framework provides clear rules for determining the filter parameters based directly on what matters: the stopband requirements. Table 1, in combination with (3), might be all that is needed, even by sensor manufacturers, in order to provide output filtering with the smallest phase drop possible.

References

1. Antoniou, A.: Digital Signal Processing. McGraw-Hill, New York (2006)
2. Åström, K.J., Wittenmark, B.: Computer-Controlled Systems: Theory and Design. Prentice Hall, New Jersey (1997)
3. Bogart, T.F., Beasley, J.S., Rico, G.: Electronic Devices and Circuits. Prentice Hall, New Jersey (2001)
4. Elliott, S.: Signal Processing for Active Control. Academic Press, London (2001)
5. Franco, S.: Design with Operational Amplifiers and Analog Integrated Circuits. McGraw-Hill, New York (2002)
6. Henderson, K., Kautz, W.: Transient Responses of Conventional Filters. IRE Trans. Circuit Theory 5(4), 333-347 (1958)
7. Paarmann, L.D.: Design and Analysis of Analog Filters: A Signal Processing Perspective. Springer Science Business Media (2001)
8. Thede, L.: Practical Analog and Digital Filter Design. Artech House, Norwood (2004)
9. Thomson, W.: Delay Networks having Maximally Flat Frequency Characteristics. Proc. IEE Part III: Radio and Communication Engineering 96(44), 487-490 (1949)
10. Van Valkenburg, M.E.: Analog Filter Design. Holt, Rinehart and Winston, New York (1982)
11. Wittenmark, B., Åström, K.J., Årzén, K.E.: Computer Control: An Overview. IFAC Prof. Brief (2002)